2015 2nd International Conference on Knowledge-Based Engineering and Innovation (KBEI)
November 5-6, 2015
(Iran University of Science and Technology) – Tehran, Iran

Multi-focus image fusion in DCT domain based on correlation coefficient

Mostafa Amin Naji, Ali Aghagolzadeh
Faculty of Electrical and Computer Engineering, Babol Noshirvani University of Technology
Babol, Iran
Mostafa.Aminnaji.IR@ieee.org, Aghagol@nit.ac.ir

***Abstract*—Multi-focus image fusion is used to collect useful and necessary information from input images with different focus depths in order to create an output image that ideally has all information from input images. In this article, an efficient, new and simple method is proposed for multi-focus image fusion which is based on correlation coefficient calculation in the discrete cosine transform (DCT) domain. Image fusion algorithms which are based on DCT are very appropriate, and they consume less time and energy, especially when JPEG images are used in visual sensor networks (VSN). The proposed method evaluates the amount of changes of the input multi-focus images when they pass through a low pass filter, and then selects the block which has been changed more. In order to assess the algorithm performance, a lot of pair multi-focused images which are coded as JPEG were used. The results show that the output image quality is better than that of the previous methods.**

Keywords—multi-focus image; image fusion; DCT domain; correlation coefficient; VSN

I. Introduction

Image fusion is a process that creates a new image by gathering information and special features from multiple source images. This single image is more informative and accurate than the source images and it consists of all important information of the source images. There is a limited depth of focus for optical lenses of CCD/CMOS cameras; so it is difficult to take a suitable photo that consists of all part of scene with different depth of field [1]. Therefore, some parts of picture are blurred. Visual sensor network (VSN) is a series of cameras that record images and video sequences. In VSN, there is a chance to create pictures with different depth of focus using more than one camera [2]. There are some limitations in VSN method that should be taken into consideration such as limited band width, energy consumption, and processing time. In visual sensor network, energy and band width play an important role in lifetime of sensors (cameras) which creates plenty of information compared to the other kind of sensors such as pressure and temperature sensors. According to the aforementioned features for gathering and transferring useful information, for optimizing the energy and processing time, it is important to process the local input images [3]. All these reasons point out that it is necessary to use multi-focus image fusion. A lot of researches have been conducted for image fusion in spatial domain [4-9]. In the simplest method in spatial domain, a weighted arithmetic mean of the pixel values of the source images is used [8]. This method reduces the image contrast and the output image is blurred.

The image fusion algorithms which used multi-scale transforms are very promising and common. Laplacian pyramid transform [10], gradient pyramid-based transform [11], morphological pyramid transform [12] and the premier ones, discrete wavelet transform (DWT) [13], shift-invariant wavelet transform (SIDWT) [14], and discrete cosine harmonic wavelet transform (DCHWT) [15] are some examples of image fusion methods which are based on multi-scale transform.

The methods which are based on multi-scale transform are complex and suffering from processing time and energy consumption issues. For example multi-focus image fusion based on DWT needs a lot of convolution operations; so it takes more processing time and energy. In addition, it is not very successful in edge places and creates ringing phenomenon in output image and reduces the quality of the output image. Due to the aforementioned reasons, image fusion algorithms in DCT domain have been used. Image fusion in DCT domain not only improves the image quality but also needs less energy consumption and processing time for image fusion process. Also, these methods are very efficient when images are coded in JPEG format for transmission or archiving. Since the input image format is JPEG standard, the methods which use DCT domain divide each of the source images into 8×8 blocks and then fuse the input images accordingly [16]. Recently, a lot of researches have been carried on in DCT domain such as DCT + average and DCT + contrast [17]. These methods have undesirable side effects on the output images like blurring or blocking artifact; so the output image quality is reduced. Due to problems in the previous methods, the image fusion in DCT domain which is based on variance was proposed [16]. In this method, variance is used as a criterion for evaluation of image contrast. It divides the input images into small blocks and then creates a merged output image by selecting the corresponding blocks which have larger variance. Phamila introduced DCT+AC-Max method in [18]. This method selects the blocks which have more number of higher values AC coefficient in DCT domain. This method fails in selection of the suitable focused block because the number of higher values AC

978-1-4673-6506-2/15/$31.00

coefficients as a fusion criterion is not proper when the majority of AC coefficients are zero. A recent method (DCT + Spatial Frequency) in DCT domain is introduced by Cao et al [19]. This method selects the block with the higher value of the spatial frequency computed for each block. These methods have some advantages compared to the previous methods, but sometimes an unsuitable block is selected; so the quality of the output image is reduced.

In this paper, a simple and yet efficient method is developed. In this method, the input images are passed through a low pass filter in order to obtain the artificial blurred images from input images. The proposed algorithm selects the block which has been changed more after passing them through a low pass filter. The correlation coefficient value between the input image's blocks and their corresponding artificial blurred blocks is used to measure the changes occurred in the image. When the changes are more, it means that the image has high details. So it is preferable to select the final fused image from this image. In this way, the error due to unsuitable block selection is minimized and the output image is sharper and with high quality. In addition the proposed method has some advantages such as flexibility in image fusion with different depth of focuses. The image fusion algorithm results can be improved with the various low pass filters.

This paper is arranged in 5 sections. In the second section, the correlation coefficient calculation between image blocks in DCT domain is discussed. The proposed method is introduced and explained in section 3. This new algorithm is also assessed with previous prominent algorithms with different tests in section 4. The last section concludes the paper.

II. DCT BLOCK ANALYZE

A. Discrete Cosine Transform

Two-dimensional DCT transform of N×N blocks of the image x(m, n) and its inverse DCT transform are defined as (1) and (2), respectively [16]:

$$\mathbf{d(i,j)} = \frac{2\alpha(i)\alpha(j)}{N} \times \sum_{m=0}^{N-1}\sum_{n=0}^{N-1} \mathbf{x(m,n)} \cos\left[\frac{(2m+1)\pi k}{2N}\right] \times \cos\left[\frac{(2n+1)\pi k}{2N}\right] \tag{1}$$

$$\mathbf{x(m,n)} = \frac{2}{N} \times \sum_{i=0}^{N-1}\sum_{j=0}^{N-1} \alpha(i)\alpha(j)\mathbf{d(i,j)} \cos\left[\frac{(2m+1)\pi k}{2N}\right] \times \cos\left[\frac{(2n+1)\pi k}{2N}\right] \tag{2}$$

where i, j, m, n =0,1,…, N-1 and

$$\alpha(i) = \begin{cases} \frac{1}{\sqrt{2}} & \text{if } i = 0 \\ 1 & \text{otherwise} \end{cases} \tag{3}$$

According to (1), d(0,0) is the DC coefficient and it represents the mean value of the image block. The other d(i,j) is the AC coefficients of the block.

B. The Correlation Coefficient Calculation in DCT Domain

The correlation coefficient is a statistical tool to determine the degree of linear relationship (correlation) between two variables. The correlation coefficient between the two N×N block of images A and B is defined as (4):

$$\mathbf{Corr(A,B)} = \frac{\sum_{m=0}^{N-1}\sum_{n=0}^{N-1}(\mathbf{A(m,n)} - \bar{a})(\mathbf{B(m,n)} - \bar{b})}{\sqrt{\sum_{m=0}^{N-1}\sum_{n=0}^{N-1}(\mathbf{A(m,n)} - \bar{a})^2}\sqrt{\sum_{m=0}^{N-1}\sum_{n=0}^{N-1}(\mathbf{B(m,n)} - \bar{b})^2}} \tag{4}$$

where A(m,n) is the intensity of the $(m,n)^{th}$ pixel in image A, B(m,n) is the intensity of the $(m,n)^{th}$ pixel in image B, $\bar{a}$ is the mean intensity value of image A, and $\bar{b}$ is the mean intensity value of image B.

In order to derive the correlation coefficient of N×N block of image A and B in DCT domain, the $P_A(i,j)$ and $P_B(i,j)$ are defined as below:

$$P_A(i,j) = d_A(i,j) - \bar{d}_A \tag{5}$$

$$P_B(i,j) = d_B(i,j) - \bar{d}_B \tag{6}$$

where $d_A(i,j)$ and $d_B(i,j)$ are the DCT coefficients of N×N block of image A and B, respectively. Also $\bar{d}_A$ and $\bar{d}_B$ are mean values of DCT coefficients of N×N block of image A and B, respectively.

Then, the correlation coefficient between two N×N blocks of image A and B in DCT domain is given as:

$$\mathrm{Corr_{DCT}}(A,B) = \frac{\sum_{i=0}^{N-1}\sum_{j=0}^{N-1} P_A(i,j) \times P_B(i,j)}{\sqrt{\sum_{i=0}^{N-1}\sum_{j=0}^{N-1} P_A(i,j)^2} \times \sqrt{\sum_{i=0}^{N-1}\sum_{j=0}^{N-1} P_B(i,j)^2}} \tag{7}$$

Therefore, the correlation coefficient of two N×N blocks of image A and B can be obtained simply from the DCT coefficients mathematically.

III. PROPOSED METHOD

A. Correlation Coefficient Based Image Fusion in DCT Domain

In order to simplify the proposed algorithm, two images are considered for image fusion. This algorithm can be used for more than two images. It is considered that the input images are adjusted by an image registration method. Figure 1 shows the general structure of the proposed method for two images fusion.

In the first step, the artificial blurred images are obtained from the input images by passing them through a low pass filter. The input images and their corresponding artificial blurred images are divided into 8×8 blocks and then the DCT coefficients of the blocks are calculated. The first input image block, its corresponding blurred block, the second input image block, and its corresponding blurred block are called imA, $\overline{\text{imA}}$, imB and $\overline{\text{imB}}$, respectively. It is obvious that the difference between the sharp image and its corresponding blurred image is more than between unsharp image and its corresponding blurred image. Therefore, the block that comes from a part of the focused image, changes more when it is passed through a low pass filter. Consequently the correlation coefficient value between the block of the focused image, before and after passing through a low pass filter is less than the correlation coefficient value between the block of that part of image which is blurred or not focused. Therefore, the block which is changed more after passing it through a low pass filter and so its correlation coefficient value is lower, will be selected for the output fused image.

of region in an image comes from image B but the majority of surrounding blocks come from image A, the selected block of image B is substituted by the corresponding block of image A. Li et al. in [13] used the majority filter for consistency verification. So the enhanced decision map (E_Decision_Map) was obtained by applying the lowpass filter, like averaging filter, on decision map. Finally the fused output image (DCT+Corr+CV) is created from the blocks as (10):

$$\text{output image}(\text{DCT}+\text{Corr}+\text{CV}) = \begin{cases} \text{imA} & \text{if} \quad \text{E\_Decision\_Map}(m,n) < 0 \\ \text{imB} & \text{if} \quad \text{E\_Decision\_Map}(m,n) > 0 \\ (\text{imA}+\text{imB})/2 & \text{if} \quad \text{otherwise} \end{cases} \tag{10}$$

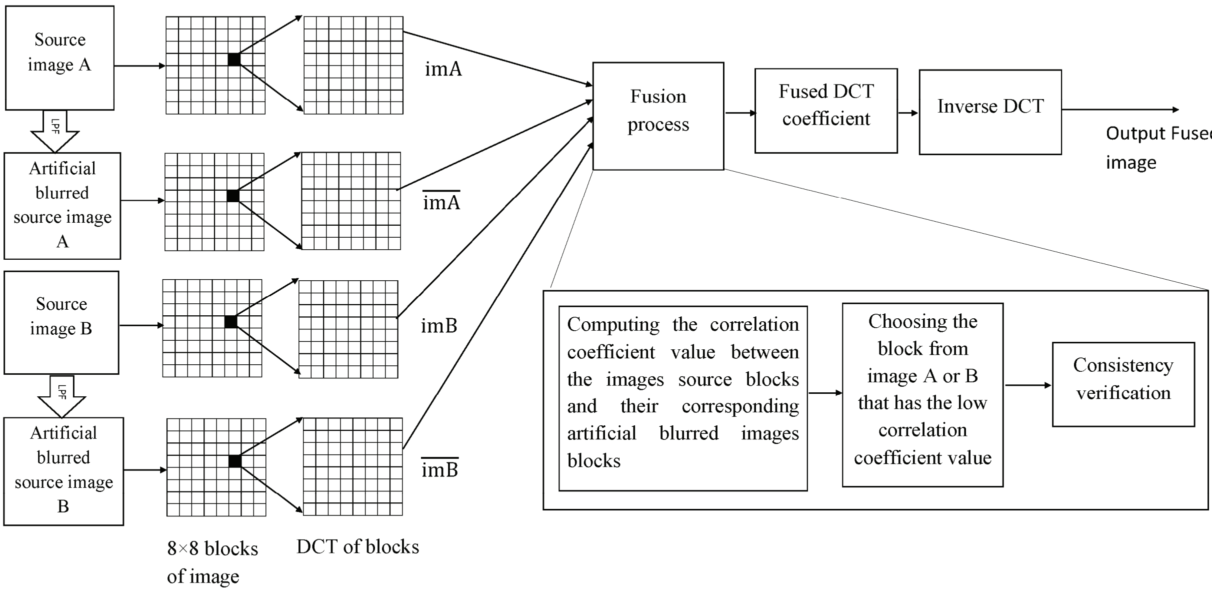

Figure 1. General structure of the proposed method.

Hence, the correlation coefficient value is used as a criterion to obtain the decision map for image fusion process as:

$$\text{Decision\_Map} = \begin{cases} -1 & \text{if} \quad \text{corr}_{\text{DCT}}(\text{imA}, \overline{\text{imA}}) < \text{corr}_{\text{DCT}}(\text{imB}, \overline{\text{imB}}) \\ +1 & \text{if} \quad \text{corr}_{\text{DCT}}(\text{imA}, \overline{\text{imA}}) > \text{corr}_{\text{DCT}}(\text{imB}, \overline{\text{imB}}) \\ 0 & \text{otherwise} \end{cases} \tag{8}$$

The block selection for the fused output image (DCT+Corr) is defined as (9).

$$\text{output image }(\text{DCT}+\text{Corr}) = \begin{cases} \text{imA} & \text{if} \quad \text{Decision\_Map} = -1 \\ \text{imB} & \text{if} \quad \text{Decision\_Map} = +1 \\ (\text{imA}+\text{imB})/2 & \text{if} \quad \text{Decision\_Map} = 0 \end{cases} \tag{9}$$

B. Consistency Verification

In order to improve the quality of the output image and reduce the error due to unsuitable block selecting, the consistency verification (CV) is applied as a post-processing after image fusion processing. It means that if the central block

IV. SIMULATION RESULTS

In this section, the results of the proposed method are discussed and they are compared with the previous methods such as the methods which are based on multi-scale transform like DWT [13], SIDWT [14], and DCHWT [15] and the methods which are based on DCT domain like DCT + Average [17], DCT + Variance [16], DCT+AC-Max [18] and DCT + spatial frequency [19].

A. lation Conditions

Simulation was done by MATLAB 2015a software. The used referenced images in Figure 2 are obtained from online database [20] and Non-referenced images "BOOK" and the simulation MATLAB code of DCT+Variance method is takes from online database [21] which provided by Haghighat [16].

For simulation DCHWT method the online database [22] is used. For the wavelet based methods, it is considered the DWT with DBSS (2,2) and the SIDWT for Haar basis with three levels of decomposition which their simulations used "Image Fusion Toolbox" provided by Oliver Rockinger [23].

In the proposed method, artificial blurred images are created from the input images using a 5×5 averaging filter. For the majority filter used in CV, an averaging mask of size 3×3 is used in two consecutive times.

Figure 2. Standard test images used for simulation.

B. Performance measurement

In order to assess the proposed algorithm with previous algorithms, evaluation performance metric of image fusion is used. The structural similarity measure (SSIM) [24], Mean-squared error (MSE) and peak signal-to-noise ratio (PSNR) [25] are used as metrics that needs ground truth image for the referenced images.

For the non-reference images with different depth focuses, when the ground truth image is not available, the total information transferred from the source images to the fused image ($Q^{AB/F}$), the total loss of information ($L^{AB/F}$), noise or artifacts added in fused image due to fusion process ($N^{AB/F}$) provided by Petrovic [26, 27] and feature mutual information (FMI) [28] are used.

C. Fusion Results Evaluation

In the first step, the proposed method was applied on ten pairs of artificial multi-focus images generated from 5 images shown in Figure 2. For each pair, the non-focused conditions created by artificial blurring of images using two disk averaging filters of radiuses 5 and 9 pixels. These images are blurred in right or left half. The average values of SSIM and MSE for the proposed and other algorithms are listed in Table I.

Our proposed method shows the best results for both with CV and without CV. In the second step, the listed algorithms are implemented on three multi-focus images to exhibit the efficiency of the proposed algorithm in fusion of more than two images.

Three multi-focus images of "Pepper" as depicted in Figure 3 (b)-(d) are produced by applying disk averaging filters of radiuses 9 on one third, in left, middle and right of "Pepper" image. The results of algorithms and the difference of the ground-truth and the fused images are shown in Figure 3. The values of performance metrics (SSIM, MSE and PSNR) for "Pepper" image are listed in Table II. The results of our

TABLE I. THE PERFORMANCE EVALUATION OF DIFFERENT ALGORITHMS FOR THE REFERENCED IMAGES

method	**Average values for Ten pairs image created from image shown in Figure 2.**	
	SSIM	***MSE***
DCT+Average [17]	0.8888	72.5253
DWT [13]	0.9514	21.2994
SIDWT [14]	0.9541	17.9557
DCHWT [15]	0.9911	4.7119
DCT+Variance[16]	0.9712	18.0685
DCT+Ac-Max[18]	0.9894	5.1054
DCT+SF [19]	0.9902	5.9870
DCT+Corr (our proposed)	**0.9970**	**3.4636**
DCT+Variance + CV [16]	0.9924	9.3907
DCT+Ac-Max + CV[18]	0.9965	1.7855
DCT+SF +CV [19]	0.9983	2.2705
DCT+Corr+CV (our proposed)	**0.9996**	**0.8526**

algorithm (SSIM=1 and MSE=0) is the same as the ground-truth image.

In the third step, the proposed algorithm and the other corresponding algorithms are assessed by a real multi-focus image with different focuses in camera.

The output fused image of the proposed and the other algorithms for "BOOK", as a non-referenced image, and their magnified version are shown in Figure 4. Evaluation performance metric $Q^{AB/F}, L^{AB/F}, N^{AB/F}$ and FMI values also are listed in Table III. The advantage of the proposed method in non-referenced image (realistic image) is also obvious.

TABLE II. THE PERFORMANCE EVALUATION OF DIFFERENT ALGORITHMS FOR THE "PEPPER" IMAGES

method	"Pepper" image data base		
	SSIM	***MSE***	***PSNR***
DCT+Average [17]	0.9342	44.5387	31.6434
DWT [13]	0.9769	13.4874	36.8315
SIDWT [14]	0.9790	12.2959	37.2332
DCHWT [15]	0.9906	5.3512	40.8463
DCT+Variance[16]	0.9456	36.8027	32.4720
DCT+Ac-Max[18]	0.9705	16.0445	36.0776
DCT+SF [19]	0.9741	16.4563	35.9675
DCT+Corr (our proposed)	**0.9944**	**0.6840**	**43.8355**
DCT+Variance + CV [16]	0.9773	28.4259	33.5931
DCT+Ac-Max + CV[18]	0.9962	5.3677	40.8329
DCT+SF +CV [19]	0.9954	5.8654	40.4479
DCT+Corr+CV (our proposed)	**1**	**0**	∞

TABLE III. THE PERFORMANCE EVALUATION OF DIFFERENT ALGORITHMS FOR THE NON-REFERENCED IMAGE

method	"BOOK" image data base			
	$Q^{AB/F}$	$L^{AB/F}$	$N^{AB/F}$	***FMI***
DCT+Average [17]	0.4985	0.5002	0.0025	0.9075
DWT [13]	0.6621	0.2294	0.3569	0.9117
SIDWT [14]	0.6932	0.2637	0.1279	0.9122
DCHWT [15]	0.6684	0.3014	0.0705	0.9123
DCT+Variance[16]	0.7210	0.2660	0.0277	0.9135
DCT+Ac-Max[18]	0.7081	0.2781	0.0294	0.9136
DCT+SF [19]	0.7151	0.2757	0.0197	0.9148
DCT+Corr (our proposed)	**0.7269**	**0.2660**	**0.0151**	**0.9158**
DCT+Variance + CV [16]	0.7267	0.2809	0.0134	0.9159
DCT+Ac-Max + CV[18]	0.7181	0.2777	0.0095	0.9157
DCT+SF +CV [19]	0.7269	0.2796	0.0080	0.9159
DCT+Corr+CV (our proposed)	**0.7304**	**0.2692**	**0.0012**	**0.9167**

V. CONCLUSION

In this paper, a simple method in DCT domain for the multi-focus images is introduced. This method uses the correlation coefficient value to measure the amount of changes occurred in the image after passing through a low pass filter. This method not only has all advantages of methods in DCT domain but also the quality of the output images is better. The performance of the proposed method was assessed with the prominent methods in DCT domain and also with well-known methods like DWT, SIDWT, and DCHWT with different test images and various assessment criteria. The proposed method shows significant advantages and improvements compared to the recent state-of-art methods.

REFERENCES

[1] W. Wu, X. Yang, Y. Pang, J. Peng, and G. Jeon, "A multifocus image fusion method by using hidden Markov model," *Optics Communications,* vol. 287, pp. 63-72, 2013.

[2] M. B. A. Haghighat, A. Aghagolzadeh, and H. Seyedarabi, "Real-time fusion of multi-focus images for visual sensor networks," in *2010 6th Iranian Machine Vision and Image Processing (MVIP).,* Isfahan, pp. 1-6, 2010.

[3] S. Soro and W. Heinzelman, "A Survey of Visual Sensor Networks," *Advances in Multimedia*, vol. 2009, 21 pages, 2009.

[4] S. Li and B. Yang, "Multifocus image fusion using region segmentation and spatial frequency," *Image and Vision Computing*, vol. 26, no. 5, pp. 971-979, 2008.

[5] P. Kaur and M. Kaur, "A Comparative Study of Various Digital Image Fusion Techniques: A Review," *International Journal of Computer Applications,* vol.114, no. 4, 2015.

[6] S. Mahajan and A. Singh, "A Comparative Analysis of Different Image Fusion Techniques," *IPASJ International Journal of Computer Science (IIJCS)*, vol. 2, no. 1, pp. 634-642, 2014.

[7] T. Zaveri, M. Zaveri, V. Shah and N. Patel, "A Novel Region Based Multifocus Image Fusion Method," *Proceeding of IEEE International Conference on Digital Image Processing (ICDIP)*, pp. 50-54, 2009.

[8] H. A. Eltoukhy, S. Kavusi, "A computationally efficient algorithm for multi-focus image reconstruction," in *Proceedings of SPIE Electronic Imaging*, vol. 5017, pp. 332–341, 2003.

[9] M. A. Mohamed and B. M. El-Den, "Implementation of image fusion techniques for multi-focus images using FPGA," *In IEEE 28th National Radio Science Conference (NRSC)*, pp. 1-11, 2011.

[10] P. J. Burt, and E. H. Adelson. "The Laplacian pyramid as a compact image code," *IEEE Transactions on Communications*, vol. 31, no. 4, pp. 532-540, 1983.

[11] V. Petrovic and C. Xydeas, "Gradient-Based Multiresolution Image Fusion," *IEEE Transactions on Image Processing*, vol. 13, no. 2, pp. 228-237, 2004.

[12] I. De and B. Chanda, "A simple and efficient algorithm for multifocus image fusion using morphological wavelets," *Signal Processing*, vol. 86, pp. 924-936, 2006.

[13] H. Li, B. Manjunath and S. Mitra, "Multisensor Image Fusion Using the Wavelet Transform," *Graphical Models and Image Processing*, vol. 57, no. 3, pp. 235-245, 1995.

[14] O. Rockinger, "Image sequence fusion using a shift-invariant wavelet transform," in *Proceedings of IEEE International Conference on Image Processing*, vol. 3, Santa Barbara, pp. 288-291, 1997.

[15] B. S. Kumar, “Multifocus and multispectral image fusion based on pixel significance using discrete cosine harmonic wavelet transform,” *Signal, Image and Video Processing*, vol. 7, no. 6, pp. 1125-1143, 2013.

[16] M. B. A. Haghighat, A. Aghagolzadeh and H. Seyedarabi, “Multi-focus image fusion for visual sensor networks in DCT domain,” *Computers & Electrical Engineerin*g, vol. 37, no. 5, pp. 789-797, 2011.

[17] J. Tang, “A contrast based image fusion technique in the DCT domain,” *Digital Signal Processing*, vol. 14, no. 3, pp. 218-226, 2004.

[18] Y. Phamila and R. Amutha, “Discrete Cosine Transform based fusion of multi-focus images for visual sensor networks,” *Signal Processing*, vol. 95, pp. 161-170, 2014.

[19] L. Cao, L. Jin, H. Tao, G. Li, Z. Zhuang and Y. Zhang, “Multi-Focus Image Fusion Based on Spatial Frequency in Discrete Cosine Transform Domain*,” IEEE Signal Processing Letters*, vol. 22, no. 2, pp. 220-224, 2015.

[20] [Online].Available: http://www.imageprocessingplace.com/root_files_V3/image_databases.htm. [Accessed: Sep- 2015].

[21] [Online].Available: http://www.mathworks.com/matlabcentral/fileexchange/51947-multi-focus-image-fusion-in-dct-domain. [Accessed: Sep- 2015].

[22] [Online].Available: http://www.mathworks.com/matlabcentral/fileexchange/43051-multifocus-and-multispectral-image-fusion-based-on-pixel-significance-using-dchwt, [Accessed: Sep- 2015].

[23] [Online]. Available: http://www.metapix.de/toolbox.htm. [Accessed: Sep- 2015].

[24] Z. Wang, A. C. Bovik, H. R. Sheikh, and E. P. Simoncelli, “Image quality assessment: from error visibility to structural similarity*,” IEEE Transactions on Image Processing*, vol. 13, no.4, pp. 600-612, 2004.

[25] Z. Wang and A. Bovik, “Mean squared error: Love it or leave it? A new look at Signal Fidelity Measures”, *IEEE Signal Processing Magazine*, vol. 26, no. 1, pp. 98-117, 2009.

[26] C. Xydeas and V. Petrovic, “Objective image fusion performance measure,” *Electronics Letters*, vol. 36, no. 4, pp. 308-309, 2000.

[27] V. Petrović and C. Xydeas, “Objective image fusion performance characterisation,” in *2009 Tenth IEEE International Conference on Computer Vision (ICCV)*, Beijing, 2005, pp. 1866-1871.

[28] M. B. A. Haghighat, A. Aghagolzadeh and H. Seyedarabi, “A non-reference image fusion metric based on mutual information of image features,” *Computers & Electrical Engineering*, vol. 37, no. 5, pp. 744-756, 2011.

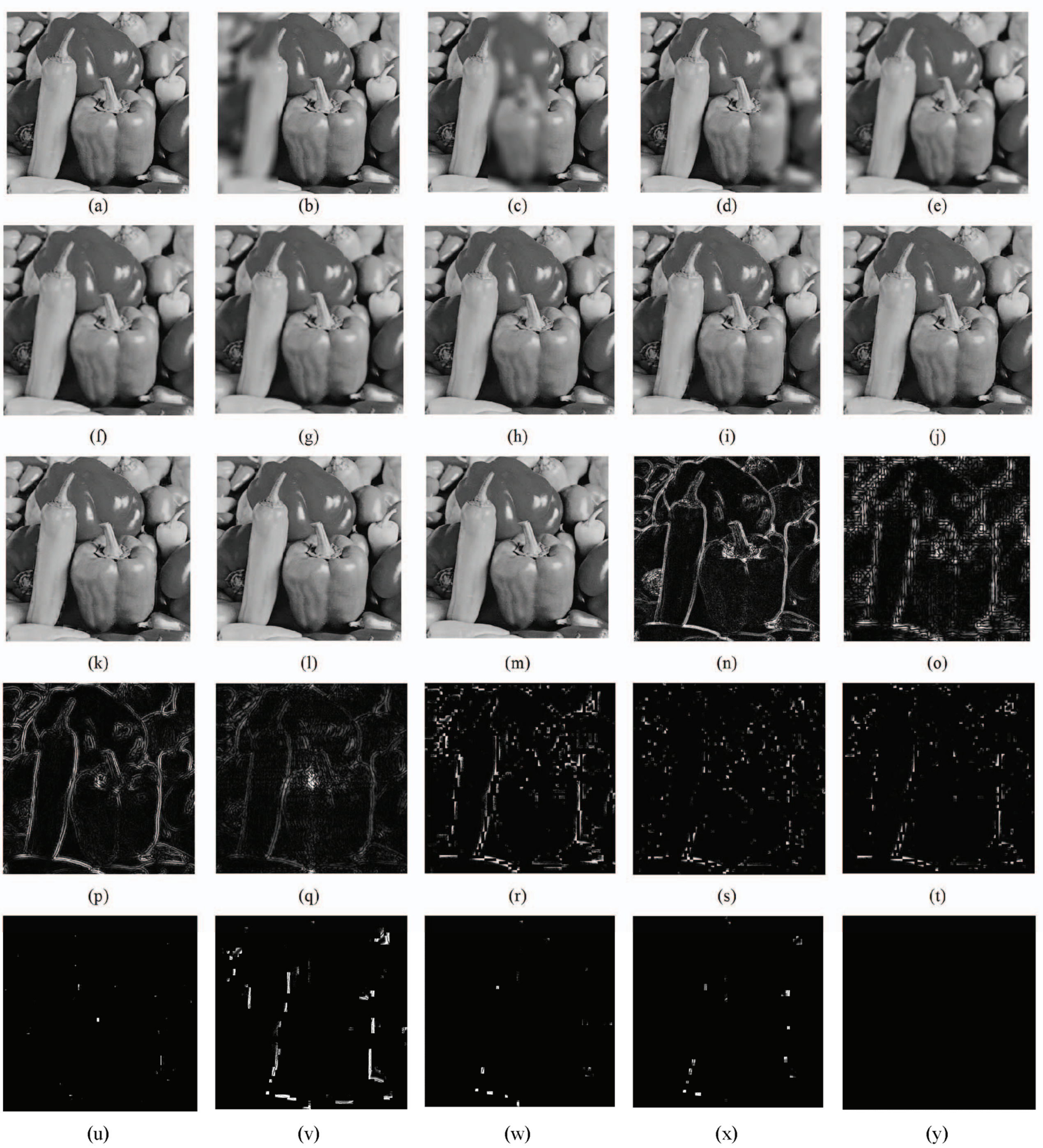

Figure 3. “Pepper” image and results of our proposed method and the other algorithms. (a) Ground-truth image. (b) First input image. (c) Second input image. (d) Third input image. (e) DCT+Average result. (f) DWT result. (g) SIDWT result. (h) DCHWT result. (i) DCT+Variance result. (j) DCT+AC-Max result. (k) DCT+SF result. (l) DCT+Corr (our proposed). (m) DCT+Corr+CV (our proposed). (n), (o), (p), (q), (r), (s), (t) and (u) are difference images between the ground-truth image and (e), (f), (g), (h), (i), (j), (k) and (l), respectively. (v), (w), (x) and (y) are difference image between the ground-truth image and the results of DCT+Variance+CV, DCT+AC_Max+CV, DCT+Spatial-Frequency+CV and DCT+Corr+CV (our proposed), respectively

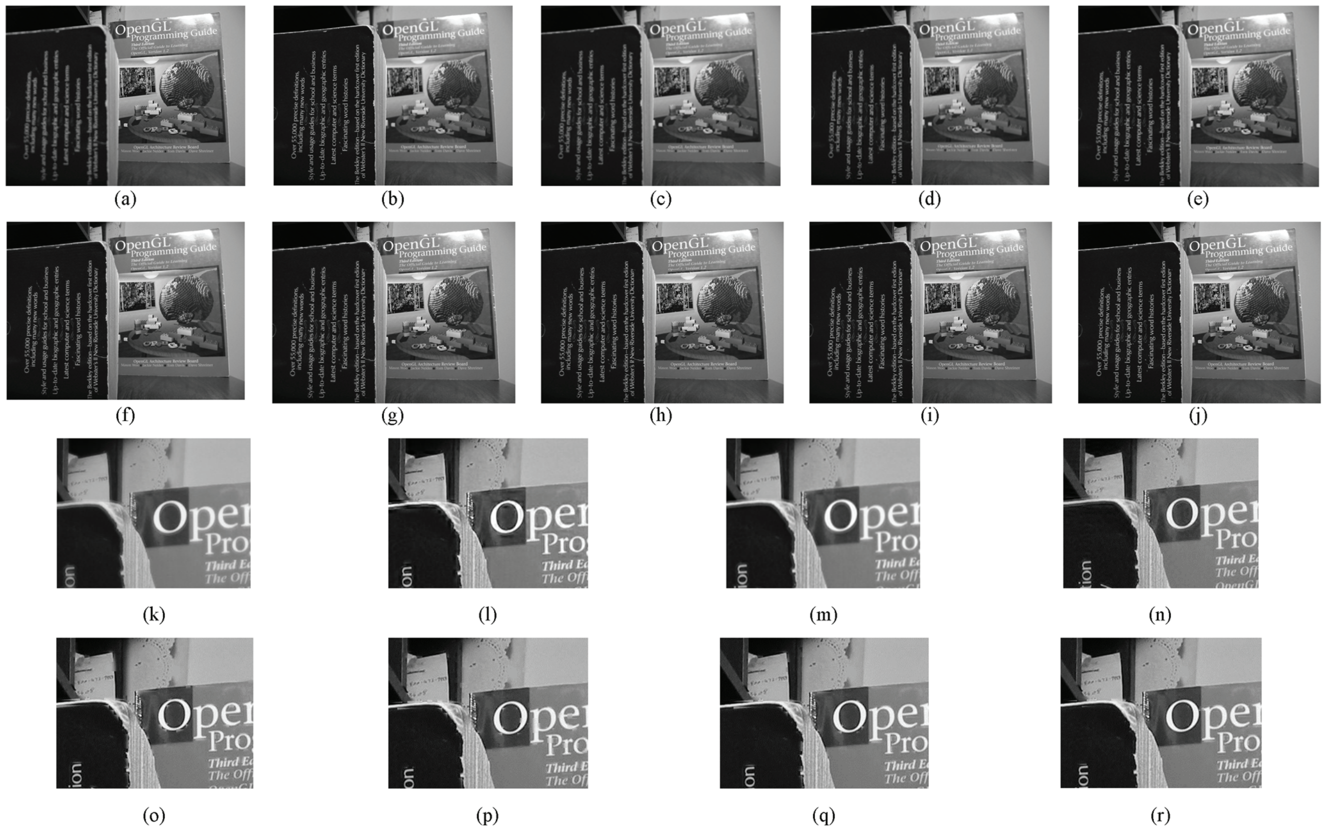

Figure 4. Source images “Book” and the fusion results. (a) The first source image with focus on the right. (b) The second source image with focus on the left. (c) DCT + Average result. (d) DWT result. (e) SIDWT result. (f) SIDWT result. (g) DCT + Variance result. (h) DCT + Ac-Max result. (i) DCT + Spatial frequency result. (j) The result of DCT + Corr (our proposed). (k), (l), (m), (n), (o), (p), (q) and (r) are the local magnified version of (c), (d), (e), (f), (g), (h), (i) and (j), respectively.